Electronic structure, magnetic behavior, and stability of Ni-P

M. R. Press, S. N. Khanna, and P. Jena

Physics Department, Virginia Commonwealth University, Richmond, Virginia 23284

(Received 1 June 1987)

Electronic-structure studies on Ni-P alloys have been carried out in order to elucidate the electronic and magnetic behavior and the stability of amorphous Ni-P glasses. Our studies invoke a mixed approach where a cluster of atoms is treated accurately through *ab initio* techniques while the remaining solid manifests itself as an effective medium. The calculated electronic density of states show general features in agreement with specific-heat and photoemission experiments. We address the issue of disappearance of magnetism in Ni-P alloys with increasing P concentration. Our studies clearly show that this disappearance of magnetism is not accompanied by a filling of the transition-metal d band. On the contrary, the number of d holes remains nearly constant while the alloy demagnetizes itself through a modification of its electronic structure induced by P p states. Our studies do not support any substantial charge transfers to or from P to Ni. We also discuss the glass-forming ability of amorphous Ni-P glass within 15–26 at. % P through realistic energy calculations.

I. INTRODUCTION

Ni-P is the most extensively studied glass, and its behavior is representative of the metal-metalloid class of glasses.[1] It is very stable in the easy glass-forming range of 15–26 at. % P with the eutectic at 19 at. % P, and shows unusually interesting properties in this range. It undergoes a transition from ferromagnetic to paramagnetic behavior around 18 at. % P,[2] and at about 23 at. % P the temperature coefficient of resistance changes from positive to negative.[3] Specific-heat[4] and Knight-shift[5] measurements indicate a decrease in the density of states (DOS) at the Fermi energy with increasing P concentration. This decrease also appears to be consistent with the observed decrease of the ir plasma frequency[6] and the conduction-electron susceptibility.[7]

The earlier theoretical picture of these glasses was based on a rigid-band description,[8,9] where it was understood that the addition of P leads to a charge transfer from P to Ni. This charge transfer causes an increase in the Fermi energy E_F. Since E_F in pure Ni lies to the right of the peak in the DOS, such a filling should lead to a decrease in the DOS at E_F with increasing P concentration and a filling of the d band. The former would explain the observed decrease in the DOS, and the latter could account for the disappearance of magnetism around 17 at. % P, if one assumed that each P atom donates three electrons to Ni. While such a picture supports rigid-band arguments, it enters into difficulties with x-ray-absorption edge and photoemission experiments[10,11] which clearly show the presence of d holes in Ni-P and related glasses at all metalloid concentrations. One is then confronted with the question of whether the d holes survive, and, if so, what is the mechanism for the loss of magnetism and a decrease in DOS at E_F with increasing metalloid concentration?

Over the past few years, several theoretical calculations using different techniques have been reported to explain this. Khanna *et al.*[12] carried out non-self-consistent Korringa-Kohn-Rostoker coherent-potential-approximation (KKR-CPA) calculations on $Ni_{74}P_{26}$ by modeling the glass as a random substitutional alloy. Their main conclusions were that the position of E_F in $Ni_{74}P_{26}$ is essentially unchanged from pure Ni; there is practically no charge transfer from metalloid to metal or vice versa and the number of d holes is nearly unchanged by alloying. Similar conclusions were reached by Ching[13] using linear combination of atomic orbitals (LCAO) calculations, which showed that the metalloid does not provide electrons to fill the metal d bands. Both the above calculations were nonspin polarized and, hence, could not address the key issue of magnetism. Recently, Jaswal[14] has carried out spin-polarized linearized muffin-tin orbital (LMTO) studies on Ni_3P structures and has argued that there is a strong charge transfer from the metalloid which gradually fills the Ni d band, and that the change in the magnetic behavior is linked to this d band filling. While the above controversy exists, there are other properties for which very little work has been done. In particular, the important question of easy glass-forming ability of metal-metalloid glasses within a given metalloid concentration remains largely unanswered.

The purpose of the present paper is to investigate the electronic structure, magnetic behavior, and stability of $Ni_{1-x}P_x$. We have used a cluster approach where a reasonably sized cluster of $Ni_m P_n$ atoms is treated exactly using the first-principles discrete-variational method[15] (DVM). To simulate the effect of the bulk material on computed properties, we embedded this cluster in a suitably chosen effective crystal potential.[16] Such an approach is useful in the study of systems with low symmetry, and its success in studying impurities and defects in transition metals and their oxides is well established.[17] One can now reliably calculate global properties such as the cohesive energy of a cluster. This enables us to

study variations in stability of $Ni_{1-x}P_x$ as a function of P concentration. To our knowledge, this is the first calculation of glass stability based on realistic energy calculations. Other local properties such as variation of the local magnetic moment and the local DOS can also be studied by choosing an appropriate model cluster wherein the near-neighbor interactions of the representative sites are included in the cluster.

A necessary input to any electronic-structure calculation is the geometry of the system, i.e., the positions of the atoms. As there are no structural models for Ni-P with varying P concentration,[18] we have carried out our studies only at those P concentrations for which a crystalline alloy phase exists. We have taken the crystalline phase as representative of the amorphous phase at the corresponding P concentration. In this work, we report studies on Ni_3P, $Ni_{12}P_5$, and Ni_2P structures. In order to investigate the effect of P on Ni magnetic moments, we have carried out model studies on an embedded 19-atom cluster representing pure fcc Ni, in which one or more Ni sites are replaced by P atoms.

In Sec. II the main features of the method employed are elaborated on; our results are presented and discussed in Sec. III, while Sec. IV is devoted to conclusive remarks.

II. THEORETICAL METHOD

A. Electronic-structure calculations

The nonrelativistic one-electron Hamiltonian for a cluster of atoms in the self-consistent spin-polarized local-density formalism[19] is given in Hartree atomic units by

$$H = -\tfrac{1}{2}\nabla^2 + V_C(\mathbf{r}) + V_{xc}^{\sigma}(\mathbf{r}) .\qquad(1)$$

The electron density $\rho(\mathbf{r})$ is expressed as a sum over molecular spin orbitals $\phi_{j\sigma}(\mathbf{r})$ with occupation $n_{j\sigma}$,

$$\rho(\mathbf{r}) = \sum_{j,\sigma} n_{j\sigma} |\phi_{j\sigma}(\mathbf{r})|^2 .\qquad(2)$$

The Coulomb potential has an electronic and a nuclear part,

$$V_C(\mathbf{r}) = \int \frac{\rho(\mathbf{r}')d\mathbf{r}'}{|\mathbf{r}-\mathbf{r}'|} - \sum_k \frac{Z_k}{|\mathbf{r}-\mathbf{R}_k|} ,\qquad(3)$$

where Z_k is the atomic number of nucleus k at a distance $|\mathbf{r}-\mathbf{R}_k|$ from the electron. The local potential for exchange-correlation, $V_{xc}^{\sigma}(r)$, is chosen to be of the spin-polarized Hedin-Lundquist[20] form. Allowing the spatial parts of the spin orbitals $\phi_{j\sigma}$ to be different for different spins leads to spin polarization, in addition to the contributions of unpaired spins.

In the DVM the molecular orbitals are expanded on a basis of numerical atomic orbitals (the LCAO approximation). Spherical potential wells around the atoms are employed to obtain more contracted valence orbitals; these include $3d$, $4s$, and $4p$ for Ni, and $3s$, $3p$, and $3d$ for P. The orbital configurations are $3d^{9.0}$, $4s^{0.99}$, and $4p^{0.01}$ for Ni, and $3s^{2.0}$, $3p^{2.99}$, and $3d^{0.01}$ for P. The secular equations $(\underline{H}-E\underline{S})\underline{C}=0$ are then solved self-consistently using matrix elements determined by three-dimensional numerical integrations performed on a random-points grid by the diophantine method.[15,21] About 600 sampling points per atom are found to be sufficient for convergence in the DOS and the eigenvalue spectrum to within 0.01 eV. In the so-called self-consistent-charge (SCC) approximation, the actual electronic density is replaced by a model density $\rho_{SCC}(\mathbf{r})$, which is a superposition of radial densities $R_{nl}^{\nu}(\mathbf{r}_\nu)$ centered on cluster atoms, via diagonal-weighted Mulliken populations A_{nl}^{ν},[22]

$$\rho_{SCC}(\mathbf{r}) = \sum_{\nu} A_{nl}^{\nu} |R_{nl}^{\nu}(\mathbf{r}_\nu)|^2 .\qquad(4)$$

The model potential derived from this density is expected to be well suited for compact periodic structure such as are present in metal compounds. For directional bonds and highly anisotropic charge distributions, however, a more exact fit to $\rho(\mathbf{r})$, obtained through a multipolar, multicenter expansion of $\rho(\mathbf{r})$, is necessary for more precise results. Finally, and importantly, an embedding scheme[16,23] is employed to simulate the effect of the rest of the microcrystal on the cluster. It consists basically of placing numerical atomic potentials at about 200 closest sites surrounding the cluster. These potentials are truncated by means of a pseudopotential to simulate orthogonality effects.

B. Heat of formation

The standard expression for the total energy in the local-spin-density approximation is

$$E_t = \sum_{\sigma} \left[\sum_i f_{i\sigma}\epsilon_{i\sigma} - \tfrac{1}{2}\int\int \frac{\rho_\sigma(\mathbf{r})\rho_\sigma(\mathbf{r}')}{|\mathbf{r}-\mathbf{r}'|}d\mathbf{r}\,d\mathbf{r}' + \int \rho_\sigma(\mathbf{r})[E_{xc}^{\sigma}(\mathbf{r})-V_{xc}^{\sigma}(\mathbf{r})]d\mathbf{r} \right] + \tfrac{1}{2}\sum_{\mu}\sum_{\nu}{}' \frac{Z_\mu Z_\nu}{R_{\mu\nu}} .\qquad(5)$$

Here, σ is the spin index, $f_{i\sigma}$ is the Fermi function, and E_{xc}^{σ} and V_{xc}^{σ} are the exchange-correlation energy and potential in the local-spin-density approximation. In a solid, the integrals are computed over a suitably chosen representative volume Ω, corresponding to a unit cell or molecular formula unit or a Wigner-Seitz cell. Total energies calculated in this fashion are typically of the order of 10^5 eV and, with the sampling schemes chosen, are

not calculated accurately enough for direct comparison of energy differences.[24] However, it is possible to extract a much more reliable and accurate binding energy E_b with respect to some reference system, say the dissociated solid,

$$E_b = E_t^{sys} - E_t^{ref} .\qquad(6)$$

Numerical noise is minimized by computing the

reference-system energy over the same volume, using the same geometry and with the same sampling grid as for the actual system. In this way, binding energies of the order of a few eV are converged to better than 0.1 eV.

The heat of formation of a compound is the difference between the total energy of a unit cell of the compound and the sum of the energies of the constituents in their standard states. In using clusters of different shapes and sizes to study the separate constituents in their respective geometries, one must confront the legitimacy of mixing energy results from different single-cluster calculations. Our experience has shown that the embedding scheme works towards making the peripheral cluster atoms "sense" a potential similar to that found in the bulk, thereby suppressing surface or cluster-size effects. Consequently, if the input specifications for all cluster calculations are uniformly maintained, the trend in derived energy quantities such as the heats of formation is expected to be preserved.

III. RESULTS AND DISCUSSIONS

A. The host Ni

We have calculated the electronic structure for the embedded $NiNi_{12}Ni_6$ cluster [see Fig. 1(a)] representing the host fcc Ni. In Fig. 2(a) we show the total DOS. The embedding atoms are neutral and are made to vary self-consistently so that their orbital populations are closest to the central atom of the cluster. Since the cluster model yields a discrete set of energy levels, these are broadened by Lorentzian functions to simulate solid-state bands. The spin-up and -down bands are normalized to a fixed peak height and not to the total number of electrons. Our cluster total DOS does not compare well with band structure calculations[25] and does not show much structure. For a cluster with inequivalent sets of atoms in different environments, it is more instructive to look at the partial DOS from individual atoms sets. Shown in Fig. 2(b) is the local DOS on the central Ni atom, which turns out to be in quite good agreement with the DOS obtained by Moruzzi et al.[25] Clearly, the central Ni atom, with its coordination shell complete, is the "best-described" atom in the cluster. This is also reflected in the magnetic moments on the cluster atoms, presented in Table I, and calculated by taking the difference between the Mulliken populations for spin-up and -down electrons. The moment on the central atom is lowest at $1.21\mu_B$ (compared to the experimental value of $0.60\mu_B$); and the moments increase outwardly. This indicates that although the moments are lower than the atomic value, the cluster is not large enough and the cluster-microcrystal coupling is not adequate to describe the collective bulk effect that reduces the magnetic moment to $0.6\mu_B$. We have experimented with other more compact atomic basis sets and crystal pseudopotentials that reduce the moments on each set of atoms by up to $0.3\mu_B$, but otherwise leave the trend of results unchanged. Guenzburger and Ellis[17] have reported similar findings in their study of bcc Fe and Ti-Fe using 15-atom clusters.

B. $Ni_{1-x}P_x$ alloys

The crystal structures for crystalline Ni_3P, $Ni_{12}P_5$, and Ni_2P were taken from the work of Wyckoff.[26] As shown in Fig. 1(b), the 16- and 17-atom clusters chosen for Ni_3P and $Ni_{12}P_5$, respectively, correspond to the most compact set of atoms representing half the unit cell. The two structures are very similar, except that $Ni_{12}P_5$ has a P atom at the center of the unit cell. For Ni_2P, the 26-atom cluster with D_{3h} symmetry contains 18 Ni atoms and eight P atoms in triangles and hexagons about
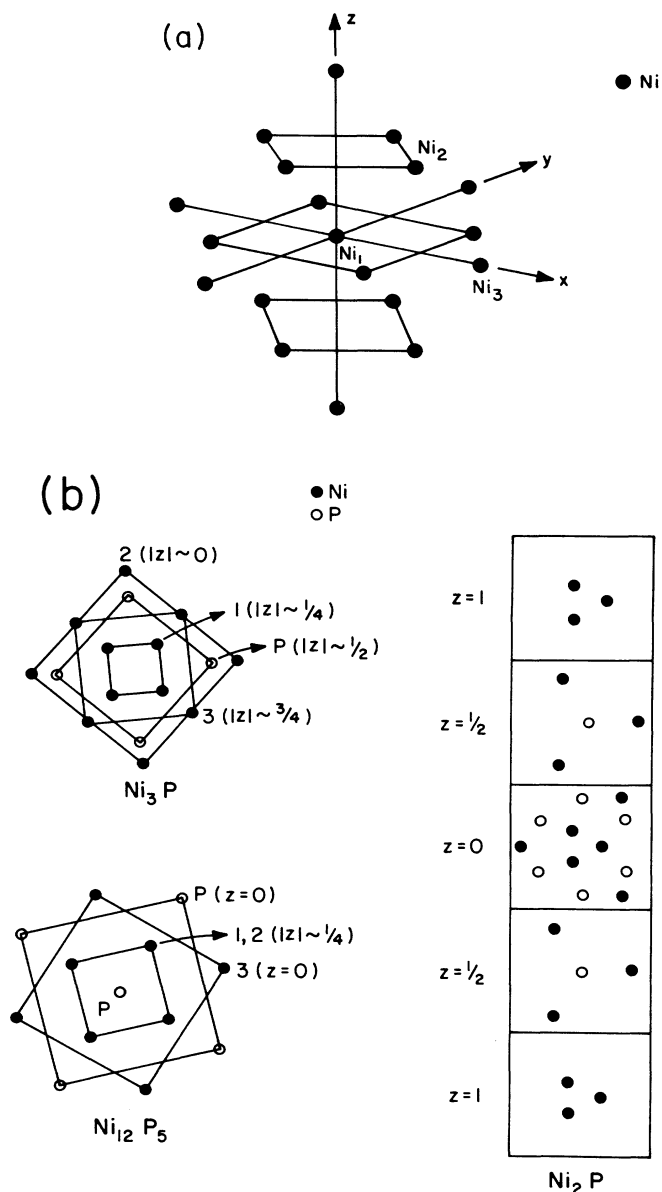
FIG. 1. (a) 19-atom fcc cluster used in model studies. (b) 16-, 17-, and 26-atom clusters representing Ni_3P, $Ni_{12}P_5$, and Ni_2P alloy structures. z corresponds to the z coordinate of the plane containing the corresponding atoms.

FIG. 3. Total density of electronic state in Ni_3P. The two curves correspond to different spin components.
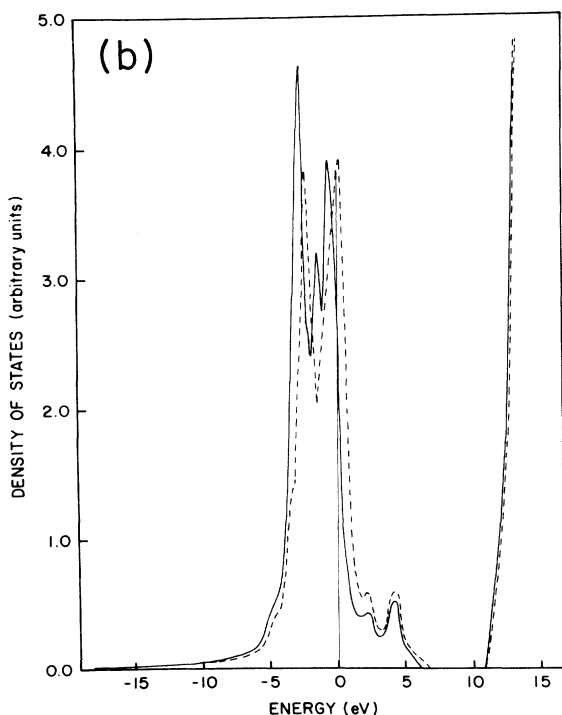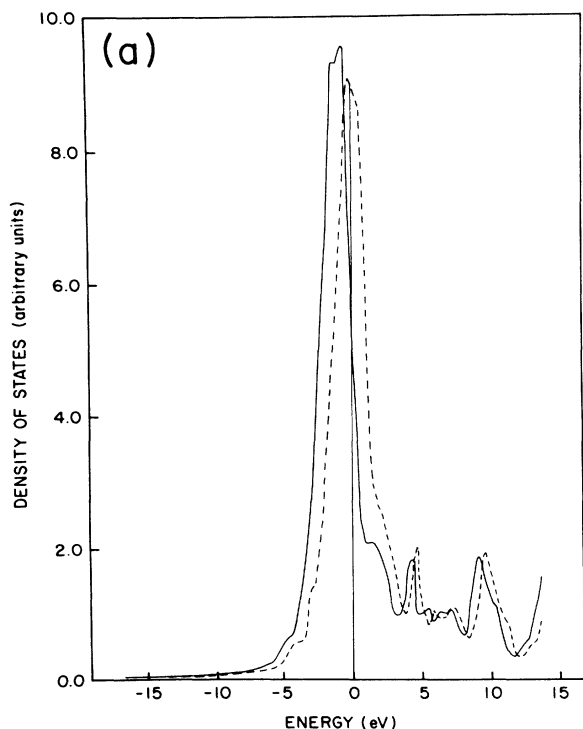
FIG. 2. (a) Total density of states for the 19-atom model cluster. The two spin components are shown by solid and dashed curves, respectively. (b) Local density of states on the central site of the 19-atom model cluster. Solid and dashed curves correspond to up and down spins, respectively.

the z axis. Although there are several kinds of Ni and P sites having different environments and coordinations in these crystals, we have taken just one Ni and one P atom in the embedding scheme. To test for the spin-moment quenching, we first allowed the orbital configurations of surrounding atoms to change with the cluster atoms. Since the Mulliken populations of the cluster atoms are quite similar to each other, we kept the crystal potential from the embedding scheme constant for all three alloys due to computational limitations. Figures 3–5 show the DOS for Ni_3P, $Ni_{12}P_5$, and Ni_2P alloys.

The main features of the alloy DOS are (i) the appearance of impuritylike states around 9.0 eV below E_F, (ii) P-induced bonding states near the bottom of the Ni d band, and (iii) the appearance of P-induced antibonding states around 7.0 eV above E_F. The position of E_F remains nearly unchanged upon alloying. These features are in good agreement with photoemission data.[11] Our calculations also indicate a decrease in the DOS per atom at E_F in the ratio 1:0.80:0.63 upon going from Ni_3P to $Ni_{12}P_5$ to Ni_2P. These values are in agreement with estimates based on specific-heat data.[4]

One of the key issues of our work is the question of magnetism in these alloys. In Table I, we give the total spin polarization at various sites in each alloy structure. It is noticed that most Ni sites have moments very close to zero; however, some Ni sites in Ni_2P and $Ni_{12}P_5$ alloys have larger moments. Apart from the cluster-size effect mentioned before, which is always present, this variation may also be attributed to the difference in local environment of these sites within the cluster. Also in
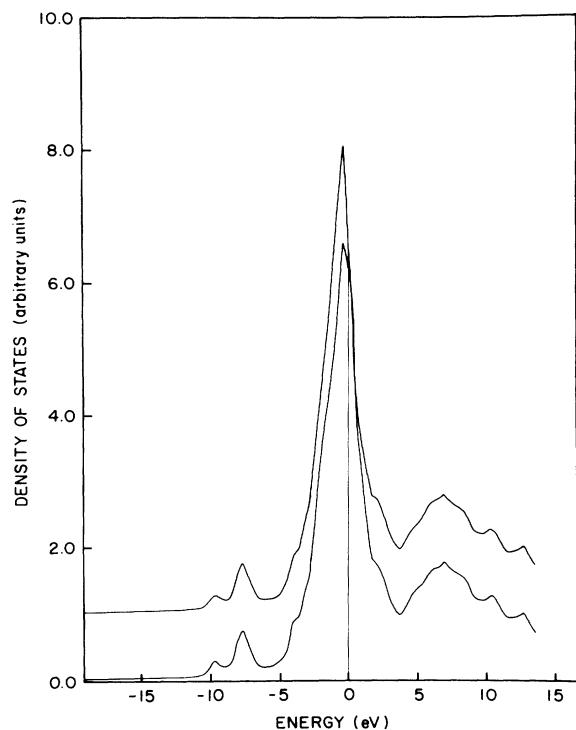
FIG. 4. Total density of electronic states in $Ni_{12}P_5$. The two curves correspond to different spin components.
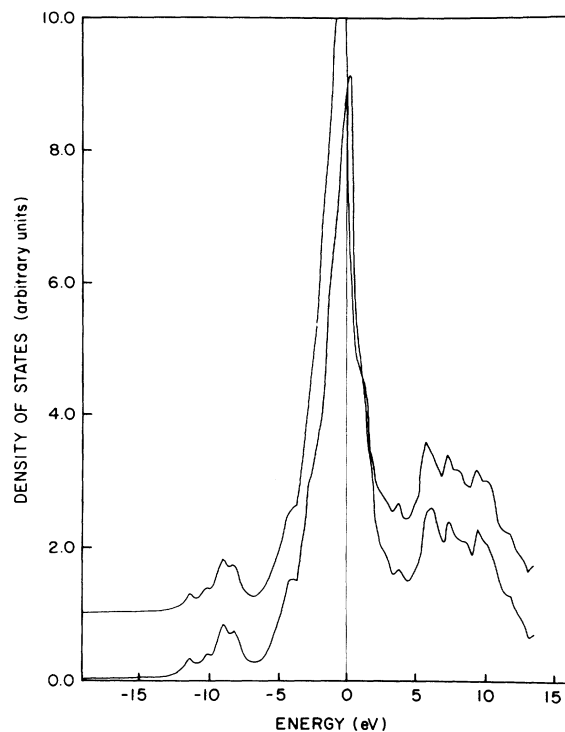
FIG. 5. Total density of electronic states in Ni_2P. The two curves correspond to different spin components.

Table I, we given, for each Ni site, its number of nearest P and Ni neighbors. Interestingly, the moment at a given site seem to be affected by the number of its P neighbors. It appears as though the P atoms quench the Ni moments and the greater the number of P neighbors, the larger the decrease in the Ni moment from its bulk

pure Ni value. In order to further investigate this quenching, we have carried out a model study. An embedded 19-atom fcc-geometry Ni cluster was selected; subsequently, the central atom, and two and four of the outermost Ni cluster atoms, were replaced by P atoms, as described in column 1 of Table II. The changes in the

TABLE I. Magnetic moments of different sites in clusters representing host Ni and $Ni_{1-x}P_x$.

System	Cluster description	Atom set	μ (μ_B)	No. of P neighbors	Mulliken ionicities
fcc Ni	$NiNi_{12}Ni_6$	Ni	1.21		
		Ni_{12}	1.25		
		Ni_6	1.59		
Ni_3P	$Ni_4Ni_4Ni_4P_4$	Ni_4 ($\|z\| = \frac{1}{4}$)	-0.01	1	$+0.18$
		Ni_4 ($\|z\| = 0$)	0.00	1	-0.16
		Ni_4 ($\|z\| = \frac{3}{4}$)	0.01	1	-0.15
		P_4 ($\|z\| = \frac{1}{2}$)	0.00		$+0.13$
$Ni_{12}P_5$	$Ni_4Ni_4Ni_4P_4P$	Ni_4 ($z = \frac{1}{4}$)	-0.06	4	$+0.10$
		Ni_4 ($z = -\frac{1}{4}$)	-0.03	2	-0.01
		Ni_4 ($z = 0$)	0.36	1	-0.12
		P_4 ($z = \frac{1}{2}$)	-0.03		$+0.03$
		P (0,0,0)	0.01		$+0.02$
Ni_2P	$Ni_3Ni_3Ni_6Ni_6$	Ni_3 ($z = 0$, in)	-0.06	4	$+0.51$
	P_6P_2	Ni_3 ($z = 0$, out)	0.56	2	-0.31
		Ni_6 ($z = \pm\frac{1}{2}$)	0.20	3	$+0.20$
		Ni_6 ($z = \pm 1$)	0.94	1	-0.23
		P_6 ($z = 0$)	-0.02		0.00
		P_3 ($z = \pm\frac{1}{2}$)	-0.14		-0.22

TABLE II. Magnetic moments and Ni d-band spin populations of different sites in model clusters obtained by replacing one, two, and four Ni atoms in a 19-atom fcc Ni cluster by P atoms.

Cluster description	Atom set[a]	Calc. μ (μ_B)[b]	No. of P nearest neighbors	Ni $d\uparrow$	Ni $d\downarrow$
Ni-Ni$_{12}$N$_6$	Ni	1.21		4.93	3.67
	Ni$_{12}$	1.25		4.86	3.66
	Ni$_6$	1.59		4.91	3.59
P-Ni$_{12}$Ni$_6$	P	-0.13			
	Ni$_{12}$	1.02	1	4.80	3.75
	Ni$_6$	1.47		4.91	3.60
Ni(Ni$_8$Ni$_4$)(Ni$_4$P$_2$)	Ni$_8$	0.91	1	4.74	3.82
	Ni$_1$	1.22		4.91	3.65
	Ni$_4$	0.96		4.79	3.75
	Ni$_4$	1.31		4.89	3.64
	P$_2$	-0.10			
Ni(Ni$_4$Ni$_8$)(Ni$_2$P$_4$)	Ni$_4$	0.70	2	4.59	3.97
	Ni$_8$	0.87	1	4.72	3.82
	Ni$_1$	1.20		4.89	3.67
	Ni$_2$	1.21		4.86	3.69
	P$_4$	0.01			

[a]Atom sets are ordered by increasing distance from P atoms.
[b]Contributions from $3d$, $4s$, and $4p$ electrons.

moments on the various Ni sites, as more and more Ni atoms are replaced by P atoms, are summarized in Table II. It is clear that the reduction in the moment on a Ni site is directly related to the number of nearest P neighbors; the effect is less pronounced on Ni sites at further distances from the P. One can now ask as to the mechanism of this decrease. In columns 5 and 6 of Table II, we give the number of up- and down-spin electrons in the d band of Ni sites as a function of the number of their P neighbors. The net contribution to the spin moments from the s and p Ni orbitals is $<0.05\mu_B$. We see that the effect of P neighbors is to displace majority-spin
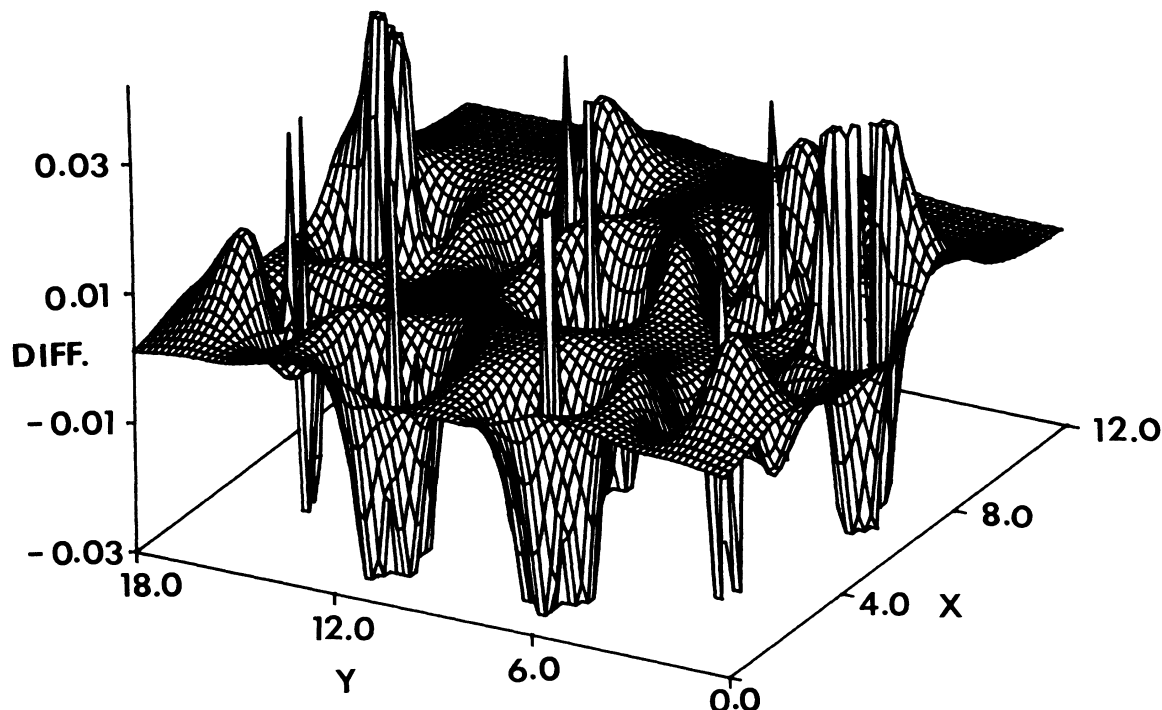
FIG. 6. The difference electronic charge density, $\rho - \rho_{SCC}$, in the $Z=0$ plane of Ni$_2$P. ρ_{SCC} is the charge density obtained through a simple superposition of atomic charge densities while ρ is the actual charge density.

electrons to minority-spin states while maintaining the total number of d electrons nearly constant to within ± 0.05 electrons. Thus, disappearance of magnetism in $Ni_{1-x}P_x$ need not imply a filling of the d- band.

The actual mechanism[27] is somewhat similar to that proposed by Friedel and Malozemoff et al. One can think of the P p states as interacting with Ni d states and forming bonding and antibonding pd hybrids. Whereas the bonding hybrids lie in the filled valence region, the antibonding hybrids lie above E_F. To accommodate the total charge, some charge must migrate to the antibonding hybrids and, since E_F is below the latter, the charge is accommodated in empty states near the Fermi energy which are mainly minority-spin states. This sets up a mechanism by which majority-spin charge gets transferred to minority-spin states due to p-d mixing. At some finite p concentration this transfer leads to a situation where it is no longer profitable for the system to polarize and the alloy becomes nonmagnetic. For the three alloys studied here, the best-described Ni sites have moments very close to zero, in agreement with experiment. To end this discussion, we point out that for Ni_3P our calculations show negligible moments on all Ni sites having even just one P neighbor within the cluster. We suspect that these results show the effect of geometry on moment formation; it appears that this structure does not support magnetic sites.

One quantitative measure of the charge transfer in these alloys is to look at the Mulliken ionicities that we have tabulated in the last column of Table I. They indicate a net charge transfer of less than 0.5 electrons to or from the metal. If one looks only at the best-described atoms in the clusters, the net charge flow is consistently small and from Ni to P; for the peripheral atoms this trend does not always hold. Another method of defining the degree of charge transfer is to look at integrated Wigner-Seitz volume charges. To this effect, we have plotted in Fig. 6 the difference electronic charge density $(\rho \text{-} \rho_{SCC})$ in the $z = 0$ plane in Ni_2P; it is representative of the charge density in the range of P concentrations studied here. It shows buildups and valleys of charge in the Ni—P bond region. Thus, what particular volume is allotted to each atom would critically determine the total charge within, thereby rendering the magnitude and direction of charge flow a nonunique result.

We now consider the question of stability of the Ni-P glass. While glass formation is a kinetic process involving liquid quenching, insight into why the glass is formed only within 15-25 at. % metalloid can be gained by looking into the total energy of the alloy as a function of P concentration. In the absence of real amorphous structures, we have determined the heat of formation for the alloy structures considered above. Our results are summarized in Table III, where the cohesive energies per cell have been multiplied by appropriate factors so as to correspond to a cell of 24 Ni atoms. One notices that

TABLE III. Cohesive energies per unit cell (E_c) and heats of formation per atom (ΔH) for Ni-P alloys.

	E_c (eV per unit cell) (24 Ni atoms)	ΔH (eV/atom)
Ni_3P	292.3	1.2
$Ni_{12}P_5$	317.7	1.4
Ni_2P	310.1[a]	0.7

[a] 4 times the unit cell.

all three structures have heats of formation of about 1 eV/atom. It is the occurrence of these highly stable crystalline phases starting at 25 at. % P which, in our view, prevents the formation of amorphous structures beyond this P concentration.

IV. CONCLUSIONS

To conclude, our studies do not support any appreciable charge transfer between Ni and P in Ni-P alloys. Figure 6 shows that the bonding charge between Ni and P atoms is fairly spread out and we believe that the large charge transfers reported by some earlier workers[14] are due to the choice of smaller volumes of space attributed to P atoms. The role of metalloids in metal-metalloid glasses is not to act as donors of charge, but to interact more closely with transition-metal states and produce changes in the electronic spectrum. The magnetic behavior is just a consequence of this electronic-spectrum change, which occurs in a manner so as to convert majority-spin electrons to minority-spin electrons, preserving overall charge neutrality.[28] Concerning glass-forming ability, we have shown that the stable crystalline phases beyond 25 at. % P prevent glass formation beyond this concentration.

In this work we have modeled the glass by an ordered alloy at the corresponding P concentration. Our studies, therefore, ignore any effects due to spatial disorder. In the next extension of this work we plan electronic-structure studies on actual disordered alloys. The atomic positions will be generated via a Monte Carlo numerical simulation using realistic pair potentials. These results will be communicated in a planned forthcoming paper.

[1]S. R. Nagel, in *Advances in Chemical Physics,* edited by I. Prigogine and S. A. Rice (Wiley, New York, 1982), Vol. **51**, p. 227; S. W. McKnight, A. K. Ibrahim, A. Bansil, and S. N. Khanna, J. Phys. F **17**, 1167 (1987); D. Nguyen Manh, D. Pavuna, F. Cyrot-Lackmann, D. Mayou, and A Pasturel, Phys. Rev. B **33**, 5920 (1986).

[2]W. A. Hines, K. Glover, W. G. Clark, L. T. Kabacoff, C. U. Modzelewski, R. Hawegawa, and P. Duwez, Phys. Rev. B **21**, 3771 (1980).

[3]J. P. Carini, S. R. Nagel, L. K. Varga, and T. Schmidt, Phys. Rev. B **27**, 7589 (1983).

[4]Y. S. Tyan and L. E. Toth, J. Electron. Mater. **3**, 791 (1974).

[5]D. S. Lashmore, L. H. Bennet, H. E. Schone, P. Gustafson, and R. E. Watson, Phys. Rev. Lett. **48**, 1760 (1982).

[6]S. W. McKnight and A. K. Ibrahim, Phys. Rev. B **29**, 6570 (1984).

[7]I. Bakonyi, L. D. Varga, A. Lovas, E. Toth-Kadar, and A. Solyóm, J. Magn. Magn. Mater. **50**, 111 (1985).

[8]S. R. Nagel and J. Tauc, Phys. Rev. Lett. **35**, 380 (1975).

[9]D. A. Pease, G. H. Hayes, M. Choi, J. I. Budnick, W. A. Hayes, R. Hasegawa, and S. M. Heald, J. Non-Cryst. Solids **62**, 1359 (1984).

[10]E. Belin, C. Bonnelle, J. Flechon, and F. Machizaud, J. Non-Cryst. Solids **41**, 219 (1980); E. Belin, D. Fargues, C. Bonnelle, J. Flechon, F. Machizaud, and J. Rivory, J. Phys. (Paris) Colloq. **41**, C8-427 (1980).

[11]A. Amanou, D. Aliaga-Guerra, P. Panissod, G. Krill, and R. Kuentzler, J. Phys. (Paris) Colloq. **41**, C8-396 (1980).

[12]S. N. Khanna, A. K. Ibrahim, S. W. McKnight, and A. Bansil, Solid State Commun. **55**, 223 (1985).

[13]W. Y. Ching, Phys. Rev. B **34**, 2080 (1986).

[14]S. S. Jaswal, Phys. Rev. B **34**, 8937 (1986).

[15]D. E. Ellis and G. S. Painter, Phys. Rev. B **2**, 2887 (1970).

[16]G. A. Benesh and D. E. Ellis, Phys. Rev. B **24**, 1603 (1981).

[17]Diana Guenzburger and D. E. Ellis, Phys. Rev. B **31**, 93 (1985); **31**, 1514 (1985).

[18]R. Harris and L. J. Lewis, Phys. Rev. B **25**, 4997 (1982); J. Phys. F **13**, 1359 (1983).

[19]P. Hohenberg and W. Kohn, Phys. Rev. **136**, B864 (1964); W. Kohn and L. J. Sham, Phys. Rev. **140**, A1133 (1965).

[20]L. Hedin and B. I. Lundquist, J. Phys. C **4**, 2064 (1971); V. von Barth and L. Hedin, *ibid.* C **5**, 1629 (1972).

[21]D. E. Ellis, Int. J. Quantum Chem. **S2**, 35 (1968).

[22]R. S. Mulliken, J. Chem. Phys. **23**, 1833 (1955); **23**, 1841 (1955).

[23]M. R. Press, Ph.D. thesis, Northwestern University, 1986.

[24]B. Delley, D. E. Ellis, A. J. Freeman, E. J. Baerends, and D. Post, Phys. Rev. B **27**, 2132 (1983).

[25]V. L. Moruzzi, J. F. Janak, and A. R. Williams, *Calculated Electronic Properties of Metals* (Pergamon, New York, 1978).

[26]R. W. G. Wyckoff, *Crystal Structures,* 2nd ed. (Interscience, New York, 1963), Vols. 1 and 2.

[27]J. Friedel, Nuovo Cimento Suppl. **3**, 287 (1958); also see *Metallic Solid Solutions,* edited by J. Friedel and A. Guinier (Benjamin, New York, 1963); A. P. Malozemoff, A. R. Williams, K. Terakura, V. L. Moruzzi, and K. Fukamichi, J. Magn. Magn. Mater. **35**, 192 (1983).

[28]C. D. Gelatt, Jr., A. R. Williams, and Y. L. Moruzzi, Phys. Rev. B **27**, 2005 (1983).